Effect of steel reinforcement on electrical measurements on concrete

Marie Antoinette Alhajj, Géraldine Villain, Sérgio Palma Lopes

Effect of steel reinforcement on electrical measurements on concrete

Marie Antoinette Alhajj, Géraldine Villain, Sérgio Palma-Lopes

IFSTTAR, Centre de Nantes, 44 344 Bouguenais, France

Contact: marie-antoinette.alhajj@ifsttar.fr

Abstract

Concrete is a construction material known for its resistance to compression and its durability. There are several methods for evaluating the durability of reinforced concrete structures, falling into two categories: destructive (D) and non-destructive (ND) methods. The DC-electrical resistivity method is devoted to ND evaluation. By measuring sets of concrete apparent resistivities, that are sensitive to water content, the durability of concrete can be evaluated. However, when applying this measurement technique to reinforced concrete structures, the measured apparent resistivity may be highly influenced by the steel reinforcement. The aim of this article is to study the influence of reinforcements on resistivity measurements on concrete. The problem was first studied using numerical analysis, then two applications were considered: the first is based on an experimental campaign and the second is an application to megastructures.

Keywords: steel reinforced concrete; durability; non-destructive testing; electrical resistivity; numerical modelling.

1 Introduction

Durability of concrete is a remarkable property of this construction material. Despite the penetration of aggressive agents like chlorides in seawater, concrete is capable of resisting to these attacks [1]. However, durability of concrete is affected by the aggressive agents and decreases when their penetration is important. For instance, the service life of a structure is reduced when it is subjected to chemical ingress [2]. Therefore, assessing the durability of concrete is necessary.

Several methods can be used and the non-destructive methods are recommended for having many advantages [3]. This study handles a method based on DC- electrical resistivity. The electrical resistivity of concrete, being sensitive to the water content, can be determined in order to evaluate the durability of concrete [4], [5]. However, electrical measurements are disturbed by the presence of steel reinforcement in concrete structures [6], [7] due to the superior electrical conductivity of steel by several orders of magnitude compared to concrete.

Megastructures, such as high-rise buildings and nuclear power plants, need to be highly reinforced. Therefore, if we want to survey them as other reinforced concrete structures, it is even more important to study the influence of the reinforcement bars (rebars) on resistivity.

To determine the effect of steel reinforcement on electrical resistivity of concrete, the problem was

studied using numerical analysis. Electrical measurements were calculated numerically in reinforced slabs for different conditions.

Firstly, this paper introduces a brief description of the electrical method. Secondly, a parametric numerical study of the influence of steel reinforcement on apparent resistivity measurements on concrete is presented. Thirdly, an experimental campaign using this method is described. Finally, the numerical modelling for this experimental campaign and an application to megastructures are presented.

2 Concrete electrical resistivity measurement

In this section, the DC-resistivity method is described. Firstly, the electrical resistivity of concrete is defined. Then, measurement principles and device are presented. Finally, the effect of steel rebars on the measurements is discussed.

2.1 Electrical resistivity of concrete

The electrical resistivity of concrete, noted ρ, is an intensive (bulk) property of the material expressing its ability to oppose the flow of free electric charges when it is subjected to an electric field. In a homogeneous and isotropic material, it is expressed by an Ohm's law ratio of the measured voltage drop V [V] to the applied current intensity I [A], multiplied by a geometric factor G [m], which is given by equation (1) [8]:

$$\rho = G\frac{V}{I} \qquad (1)$$

The electrical resistivity of concrete depends on other properties of the material related to its formulation and state [9] [10]. For instance, it is influenced by the water content in concrete [11]. Therefore, the measurement of the electrical resistivity of concrete can be used to determine the water content in concrete and consequently assess its durability.

The resistivity measurement principle consists of transmitting a direct current into concrete by means of two electrodes, and measuring induced potential drops between one or more other pairs of electrodes. Then, by applying equation (1), a so-called 'apparent' resistivity can be calculated. Since concrete is usually not homogeneous, the latter observable is not the 'true' resistivity of concrete but rather an integrated value over a volume depending on the electrode array configuration and size [12].

2.2 Electrical resistivity tomography (ERT)

Many configurations exist to measure apparent resistivities on concrete. The one presented in this study is the popular Wenner configuration [13]. The measuring device shown in Figure 1 consists of a multi-electrode resistivity probe formed by 14 electrodes equally spaced every 20 mm [14]. For all possible electrode combinations following the Wenner configuration, measurements can be performed on concrete with four different electrode spacings, noted hereafter "a" (20, 40, 60 and 80 mm) leading to four depths of investigation. This acquisition process yields a dataset consisting of 26 apparent resistivities. Subsequently, an inversion procedure is needed to reconstruct the 'true' resistivity distribution in concrete. In this study, the free software Res1D® [15] is used in order to retrieve 'true' resistivity profiles with depth in cover concrete.

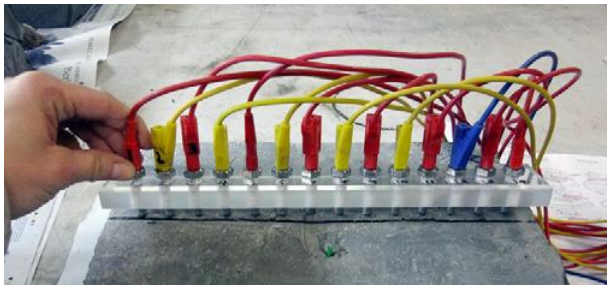

Figure 1. Concrete resistivity probe developed by du Plooy et al. (2013).

2.3 Influence of steel reinforcement

Electrical resistivity tomography (ERT) is a useful method for assessing concrete state within a range of investigation depths. However, the majority of concrete structures are reinforced with steel rebars arranged in meshes embedded within the structure. When the rebars are within the investigated volume of a given electrode array, for instance at a concrete cover thickness of 30 mm, a disturbance in the measured apparent resistivity is observed. Steel being more

conductive than concrete by many orders of magnitude, rebars may produce a significant decrease in the measured apparent resistivity [6]. Many approaches tried to minimize the perturbation of the measurements in such a case by placing the electrodes at a certain distance from the steel bars [7].

This study aims to quantify the effect of the reinforcement on the resistivity measurements. To this purpose, apparent resistivity measurements were numerically simulated in reinforced concrete structures for a range of slab geometries and positions of the electrodes.

3 Numerical simulation

This section presents the numerical study carried out by means of the finite element software, COMSOL Multiphysics® for solving the Poisson's law governing the DC-electrical problem. Apparent resistivity measurements on concrete are simulated by taking into account the presence of steel rebars near the electrode array within a 3-dimensional (3D) model.

3.1 Preliminary study

Firstly, a simple case is studied. To visualise the effect of reinforcement on apparent resistivity measurements, a 3D model of a concrete slab containing a single steel rebar of diameter 12 mm, of electrical resistivity about 0.25×10^{-6} Ω.m and at a depth of 30 mm is created (Figure 2). The concrete is homogeneous with a resistivity of 100 Ω.m and the electrodes are placed on the surface of the slab and aligned right above the steel rebar axis. Then, apparent resistivities are computed for each electrode spacing.

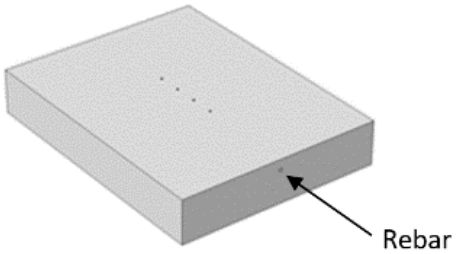

Figure 2. Model for the concrete slab with four electrodes above the single rebar

Figure 3 shows that apparent resistivity simulated for the reinforced slab model decreases as the electrode spacing increases. Indeed, as the investigation depth of the Wenner electrode array increases, the apparent resistivity becomes more sensitive to the presence of the steel rebar.

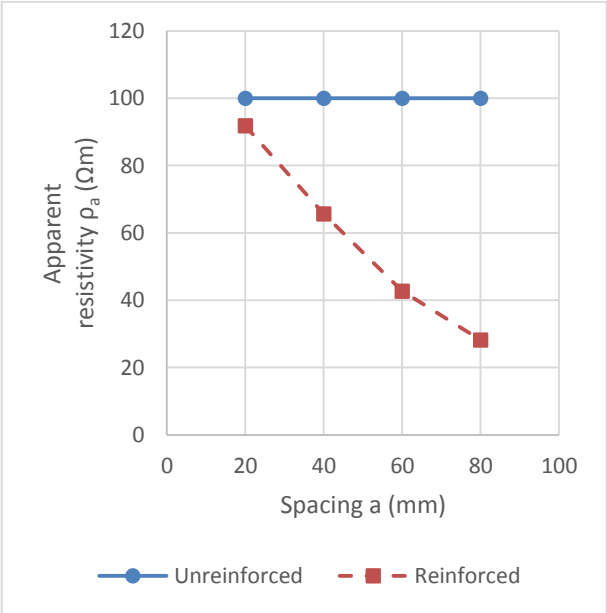

Figure 3. Apparent resistivity values for the model of unreinforced and reinforced concrete block

3.2 Parametric study

Secondly, we consider several positions of the electrodes relative to the steel rebar in the model in order to study their impact on the effect of the steel rebar.

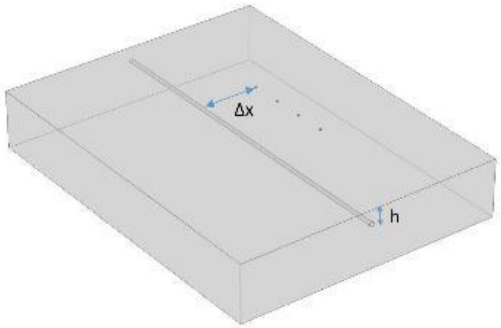

Figure 4. Schematic view of the concrete slab model (with a single rebar) showing the studied geometric parameters.

3.2.1 Effect of concrete cover thickness

The first parameter studied is the concrete cover thickness h (Figure 4). Compared to the previous result (Figure 3), the variation in apparent resistivity as a function of the electrode spacing becomes less pronounced as the cover concrete thickness increases, as shown in Figure 5. This study confirms a rather intuitive result: the lower the thickness, the closer the steel rebar to the electrode array and therefore the higher the effect of rebar on apparent resistivity.

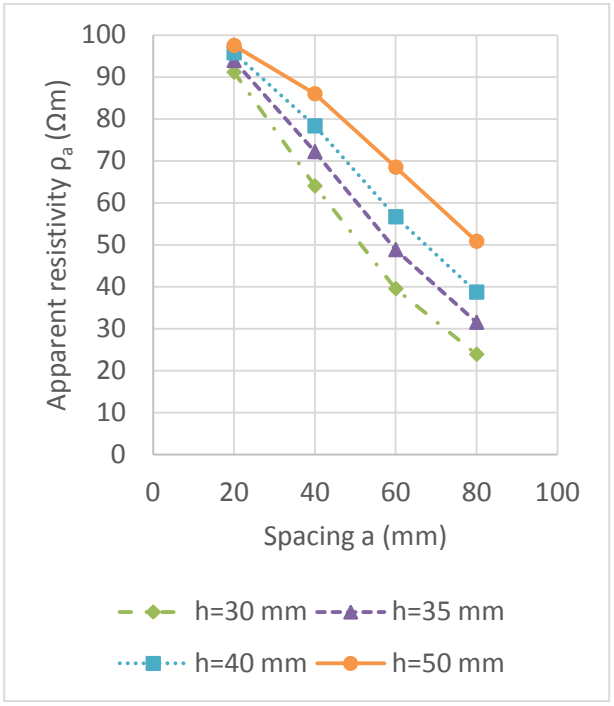

Figure 5. Variation of the simulated apparent resistivity with electrode spacing for different concrete cover thicknesses

3.2.2 Effect of the distance between the electrode line and the rebar axis

The second parameter studied is the distance between the electrode and the rebar axis Δx (Figure 4). The study of this parameter is useful in the case of megastructures. Figure 6 shows that when Δx decreases, the effect of the rebar increases, producing more significant variations in the apparent resistivity. In fact, megastructures tend to have small meshes of reinforcement, which can lead to low Δx distances, and consequently yield a higher influence of the reinforcement on measured apparent resistivities.

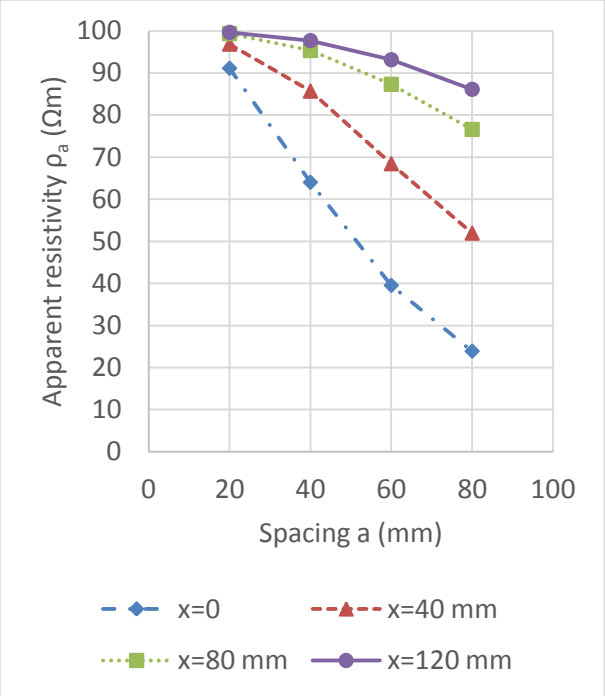

Figure 6. Variation of the simulated apparent resistivity as a function of electrode spacing for different lateral distances Δx

4 Application to an experimental campaign

The numerical study in Section 3 allowed the application to an experimental campaign that included resistivity measurements on reinforced concrete slabs.

4.1 Description of the experimental setup

The test specimens used in this paper are two concrete slabs of dimensions 900x700x150 mm^3. Both have the same concrete formulation (CEMI type C30) [16] and were both subjected to seawater ingress. One is a steel reinforced slab whereas the other is unreinforced. The reinforced slab contains four meshes of reinforcement of dimensions 200x300 mm^2 at a concrete cover thickness of 30 mm (Figure 7). The measurements on both slabs were performed on the mesh AB23 on the face subjected to the ingress of seawater.

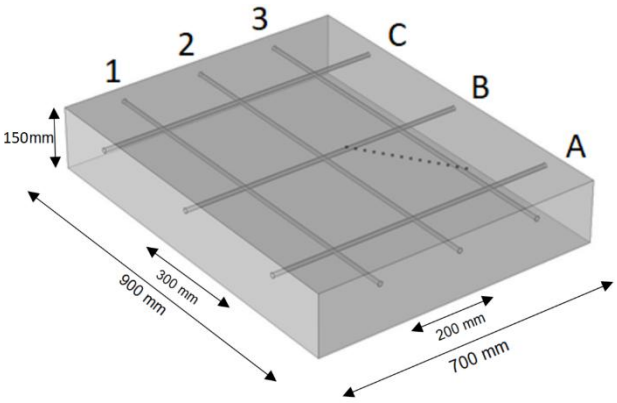

Figure 7. 3D model of the reinforced slab used in the experimental campaign and positions of the electrodes on the surface.

4.2 Experimental campaign results

The seawater ingress was monitored at different test times. This study focused on the first four test times, T1, T2, T3 and T4. For each test time, three measurements were performed on the mesh AB23 for each slab. The averaged results are shown in Figure 8. Concerning the unreinforced slab (NR), the apparent resistivity values increase with the electrode spacing a. Hence, when the investigation depth increases, the 'true' resistivity increases. This occurs because the moisture content is higher at the surface (where the measurement is carried out) than it is at depth in the concrete slab. In addition, due to the increase of seawater penetration with time, the measured apparent resistivity for each spacing decreases with time. This observation is valid for the two slabs. Comparing the two slabs at different times, the measured apparent resistivity decreases with the electrode spacing in the reinforced slab, due to the presence of the steel reinforcement. This disturbance leads the apparent resistivity values for the reinforced slab to decrease as the spacing increases (for a > 40 mm).

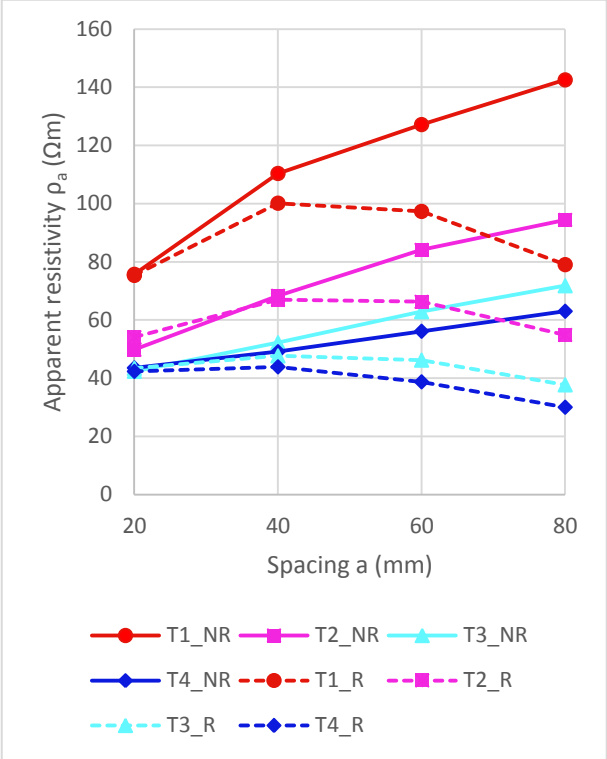

Figure 8. Measured apparent resistivity for the unreinforced and reinforced slabs of the experimental campaign, for different electrode spacings and test times

4.3 Experimental campaign modelling

A numerical modelling of these measurements was done to determine the influence of steel on the apparent resistivity measurement. Unlike the models in Section 3, the concrete in this case has a non-homogeneous resistivity distribution due to the progressive penetration of seawater.

The apparent resistivities can be calculated for each slab using the following procedure:

- inversion of measured apparent resistivities using Res1D® in order to get 'true' resistivities;
- fitting of true resistivities using Weibull curves, as proposed in [17];
- application of the fitted resistivity curves to the model instead of a constant value of resistivity.

Then, apparent resistivities are computed from a synthetic slab and compared to the measured ones. For the unreinforced slab, Figure 9 shows that the numerical results are very close to the

experimental ones for each test time and electrode spacing, which simply shows that the convergence criterion of the inversion process reached very low values for all test times and that the numerical model is valid.

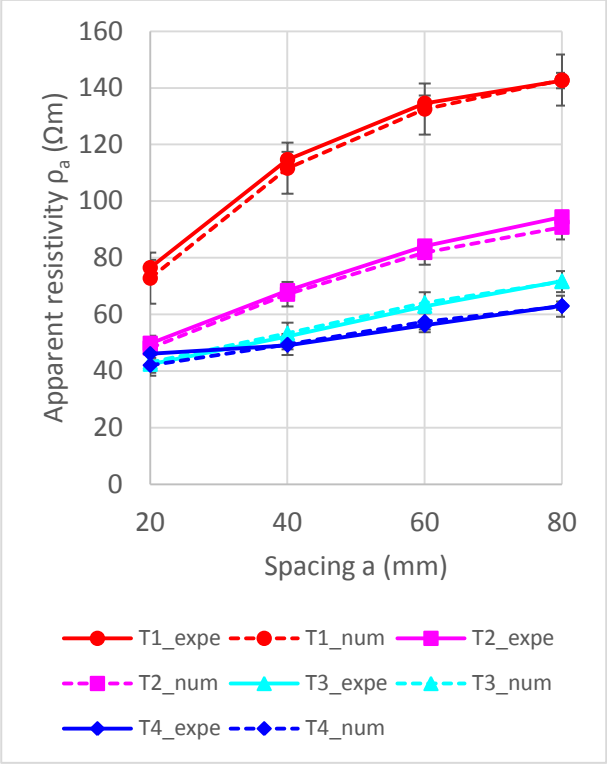

Figure 9. Measured and simulated apparent resistivity vs. spacing curves for the unreinforced slab at different test times

For the reinforced slab, the apparent resistivity curves could not be inverted due to the significant disturbance caused by the presence of steel reinforcement. Therefore, the actual resistivity profiles in the reinforced slab could not be assessed. As an alternative, the inverted resistivity profiles of the unreinforced slab were used for the reinforced slab as well, based on the assumption that the two slabs are in almost identical states. The simulated and measured apparent resistivities are compared in Figure 10. These profiles are fairly comparable, although the discrepancies between simulated and measured data are generally larger than those obtained for the unreinforced slab. This shows that our assumptions and modelling procedure for taking the steel rebar effect into account are fairly valid.

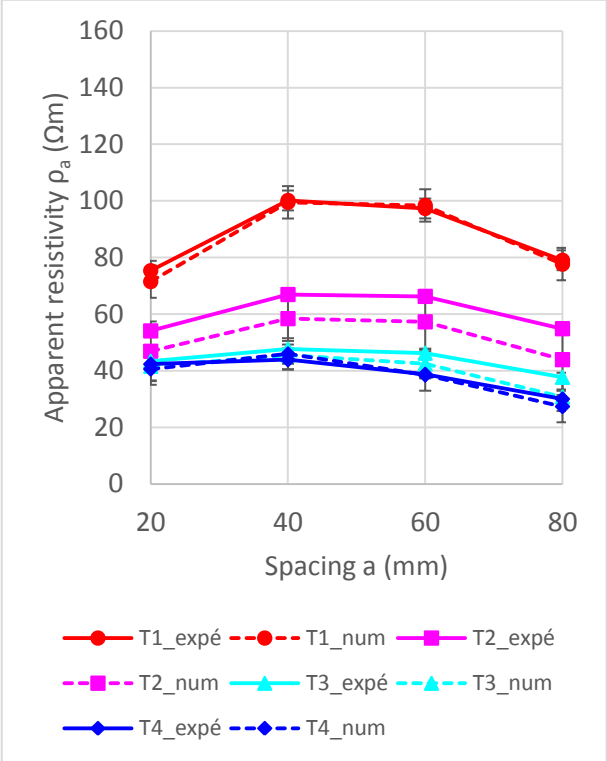

Figure 10. Measured and simulated apparent resistivity vs. spacing curves for the reinforced slab at different test times

5 Discussion and application to megastructures

Megastructures are very large built structures, such as dams, bridges, high-rise buildings, designed to be constructed on a large scale. They are characterized by high-strength concrete and finer meshes of reinforcement. Therefore, electrical resistivity measurements can be highly affected by the steel reinforcement.

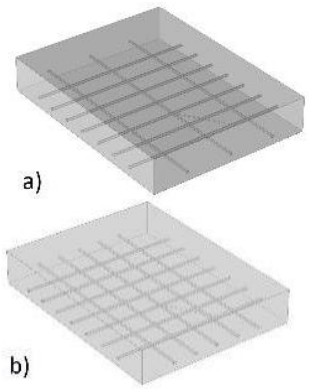

Figure 11. Model of a reinforced slab with a) 20x10 cm² reinforcement meshes and b) 10x10 cm² reinforcement meshes

To underline this effect, the model of the reinforced slab from Section 4 for the first test time T1 is used here and modified. The initial meshes of reinforcement, 20x30 cm² are reduced to 20x10 cm² then to 10x10 cm² (Figure 11). The apparent resistivities are numerically simulated for the two finer meshes and the results are shown in Figure 12. The graphs show that with finer meshes of reinforcement, apparent resistivity values are more significantly disturbed by the presence of the steel reinforcement. Moreover, this effect increases as the electrode spacing (and therefore the investigation depth) increases.

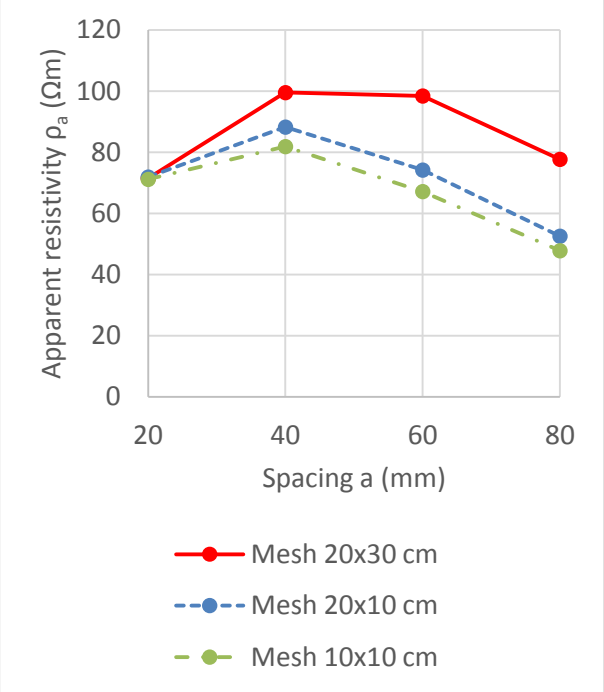

Figure 12. Simulated apparent resistivity for the reinforced slab at test time T1 with three different meshes

The percentage difference between the apparent resistivity of the mesh 20x30 cm² and the finer meshes was calculated for each electrode spacing.

Table 1 shows that the decrease of simulated apparent resistivity is more significant for higher electrode spacings and finer meshes. For instance, Δρ is higher for the smallest mesh 10x10 cm² comparing to Δρ for the mesh 20x10 cm², for all spacings. Moreover, comparing Δρ in one mesh, for example for the mesh 10x10 cm², Δρ is higher for the spacing 80 mm (32.4 %) than for the spacing 60 mm (24.6 %).

Δρ (%)	Spacing a (mm)			
Mesh	20	40	60	80
20x10	2.45	11.3	24,6	32.4
10x10	2.12	17.7	31.7	38.5

Table 1. Relative difference Δρ (%) between apparent resistivity values in the mesh 20x30 cm² and the finer meshes.

6 Conclusion

ND electrical resistivity methods may be useful techniques to assess the durability of concrete without damaging the structure. However, measurements may be significantly disturbed by the presence of steel reinforcement, which is more conductive than concrete by several orders of magnitude.

This study showed that the effect of steel rebars depends on properties related to geometry and to the positions of the electrodes. On the one hand, the more the spacing between the electrodes increases, the more the investigation volume increases, causing a stronger decrease in apparent resistivity. On the other hand, our numerical study showed that apparent resistivity values are more affected by the steel reinforcement when the cover thickness is smaller and when the array of electrode is closer to a rebar.

These results were used to model an experimental campaign, and the subsequent numerical study determined the effect of steel reinforcement in a more complex model with meshes of reinforcement.

Afterwards, a model representing smaller meshes of reinforcement, referring to the kind of meshes in high-rise buildings and megastructures, showed that the measured apparent resistivities should be

more significantly disturbed due to the presence of more finely meshed steel reinforcement.

Moreover, to obtain a more realistic numerical solution with megastructures, we can apply other resistivity profiles to the synthetic slab characterizing high-strength concrete used in megastructures.

Finally, the inversion of apparent resistivity is necessary to obtain the true resistivity distribution. Therefore, an improvement of the processing of the measurements can be done to take into account the presence of the reinforcement and its subsequent perturbation.

7 References

[1] Neville Adam M. Properties of concrete: Fourth and Final Edition. Harlow: Pearson Education Limited; 1995.

[2] Raharinaivo A, Arliguie G, Chaussadent T et al. La corrosion et la protection des aciers dans le béton. Paris : Presses de l'école nationale des Ponts et Chaussées ; 1998.

[3] Breysse D, Abraham O. Méthodologie d'évaluation non destructive de l'état d'altération des ouvrages en béton. Paris : Presse des Ponts et Chaussées ; 2005.

[4] Hammond E and Robson TD. Comparison of electrical properties of various cements and concretes. The Engineer. 1955; 199(5156):78-80 and 199(5166):114-115.

[5] Lataste JF, Villain G and Balayssac JP. Contrôle Non Destructif des bétons. Proposed book for publication at STE; 2017.

[6] Andrade C, Polder R and Basheer M. Non-destructive evaluation of the penetrability and thickness of the concrete cover. RILEM RC 189-NEC: State-of-the-Art Report; 2007.

[7] Polder RB. Test methods for on site measurement of resistivity of concrete- a RILEM TC-154 technical recommendation. Construction and Building Materials. 2001; 15:125-131.

[8] Telford WM, Geldart LP and Sheriff RE. Applied Geophysics. Cambridge: Cambridge University Press; 1990.

[9] Saleem M, Shameemt M, Hussain SE et al. Effect of moisture, chloride and sulphate contamination on the electrical resistivity of Portland cement concrete. Construction and Building Materials. 1996; 10(3):209-214.

[10] Castellote M, Andrade C and Alonso C. Measurement of the steady and non-steady-state chloride diffusion coefficients in a migration test by means of monitoring the conductivity in the anolyte chamber - Comparison with natural diffusion tests. Cement and concrete research. 2001; 31:1411-1420.

[11] Lopez W, Gonzalez JA. Influence of degree of pore saturation on the resistivity of concrete and the corrosion rate of steel reinforcement. Cement and Concrete research. 1993;23(2):368-376.

[12] Lagabrielle R. Cours de prospection électrique courant continu. École des Mines de Paris ;1997.

[13] Wenner F. A method for measuring earth resistivity. Journal of the Washington academy of sciences. 1915; 5(16):561-563.

[14] Du Plooy R, Lopes S, Villain G et al. Development of a multi-ring resistivity cell and multi-electrode resistivity probe for investigation of cover concrete condition. NDT&E International. 2013;54:27-36.

[15] Loke MH. 1-D Resistivity, IP and SIP inversion and forward modeling; 2001.

[16] NF EN 197-1. Ciment – partie 1: composition, spécifications et critères de conformité des ciments courants ; 2012.

[17] Fares M. Evaluation de gradients de teneur en eau et en chlorures par méthodes électromagnétiques non-destructives. PHD thesis. Nantes : IFSTTAR ; 2015.